BIOCHEMISTRY
including biophysical chemistry & molecular biology

Article

pubs.acs.org/biochemistry

Functionally Important Amino Acids in Rice Sucrose Transporter OsSUT1

Ye Sun,[†] Zi Lin,[‡] Anke Reinders,[†] and John M. Ward*[,†]

[†]Department of Plant Biology, University of Minnesota-Twin Cities, St. Paul, Minnesota 55108, United States

[‡]Department of Electrical and Computer Engineering, University of Minnesota-Twin Cities, Minneapolis, Minnesota 55455, United States

ABSTRACT: Six conserved, charged amino acids within membrane spans in rice sucrose transporter OsSUT1 were identified using a three-dimensional structural model based on the crystal structures of three major facilitator superfamily (MFS) proteins: LacY, GlpT, and EmrD. These positions in OsSUT1 were selected for mutagenesis and biochemical assays. Among the six mutants, D177N completely lost transport function, D331N retained only a small fraction of sucrose uptake activity (2.3% of that of the wild type), and R335H and E336Q also displayed a substantial decrease in transport activity. D329N functioned as well as wild-type OsSUT1. R188K did not transport sucrose but showed a H^+ leak that was inhibited by sucrose, indicating that R188K had uncoupled sucrose and H^+ translocation. This demonstrates that charged amino acids within membrane spans are important for the transport mechanism of OsSUT1 as they are in lactose permease.

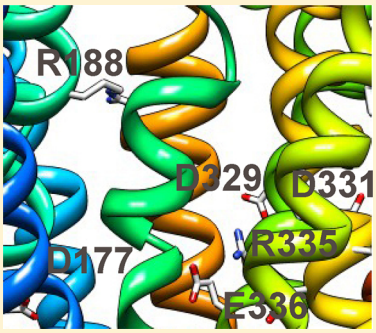

In plants, sucrose transporter proteins (SUTs, also called SUCs) are localized in the plasma membrane or vacuole membrane and couple the transport of sucrose and H^+ into the cytoplasm at a ratio of 1:1.[1−5] In many higher plants, the long-distance transport of sucrose in the phloem (vascular tissue) depends on SUTs. Mutagenesis or antisense inhibition of SUTs results in defective phloem loading of sucrose, accumulation of carbohydrates in photosynthetic leaves, and stunted growth.[6−9] In animals, SUT homologues do not function in cellular uptake but are localized to internal membranes. Human MATP (membrane-associated transport protein) is encoded by AIM1 or SLC45A2,[10,11] and mutations cause oculocutaneous albinism type 4 (OCA4). Similarly, MATP in horses is correlated with cream coat color;[12] in mice, the underwhite (uw) gene is homologous,[13,14] as well as B encoded by AIM1[15] from medaka fish. SCRT from *Drosophila* is the only homologue from animals for which transport activity has been measured.[16] SCRT was localized to internal membranes and was found to transport sucrose when expressed in yeast. Three-dimensional (3D) structures are not available for plant or animal SUTs, and key amino acids involved in the translocation mechanism remain largely unknown.[17] Only one report of mutagenesis in investigating functionally important residues exists. In that study,[18] a conserved His65 in AtSUC1 was found to interact with the inhibitor diethyl pyrocarbonate (DEPC). The H65C mutant lost sucrose transport activity, while H65K and H65R exhibited higher transport rates than the wild type.[18]

SUTs belong to the major facilitator superfamily (MFS), several members of which have been extensively studied, providing clues about the structure of SUTs. The structures of OxlT (oxalate:formate antiporter),[19] LacY (lactose:H^+ symporter),[20] GlpT (glycerol-3-phosphate:phosphate antiporter),[21] EmrD (drug:H^+ symporter),[22] and FucP (fucose:H^+ symporter)[23] show the position of substrate binding residues within the hydrophilic pore.[24] Although they vary in amino acid sequence, transported substrates, and transport coupling, these proteins share an almost identical helix arrangement and the same "alternating access" mechanism.[19−23,25] Thus, it is possible that SUTs possess a 3D structure similar to those of other MFS proteins and that known structures can be used to predict the structure of SUTs.

A striking feature of the structure/function of LacY is that only six amino acids are irreplaceable; all are charged residues, located in transmembrane helices surrounding the central cavity, and are involved in sugar binding and proton translocation.[20,26,27] Residues important for the transport activity of GlpT,[21,28] FucP,[23] and MelB[29] are mostly charged and located in the transmembrane spans. Therefore, it is reasonable to hypothesize that charged amino acids in the transmembrane helices of SUTs are essential for transport activity.

A sucrose transporter, OsSUT1 from rice (*Oryza sativa*),[30,31] was selected for this study. OsSUT1 shows large sucrose-induced currents when expressed in oocytes and is also functional when expressed in yeast.[30,31] It is the predominately expressed SUT in rice (http://plantgenomics.biology.yale.edu/riceatlas) and has been shown to be involved in seed germination, early seedling development,[32,33] and long-distance assimilate transport.[34] In this paper, we generated a 3D structural model of OsSUT1 based on a multiple-template alignment to predict functionally important amino acids. Site-directed mutagenesis, heterologous expression, and electrophysiology were used to demonstrate that five charged amino

Received: December 30, 2011
Revised: March 28, 2012
Published: March 29, 2012

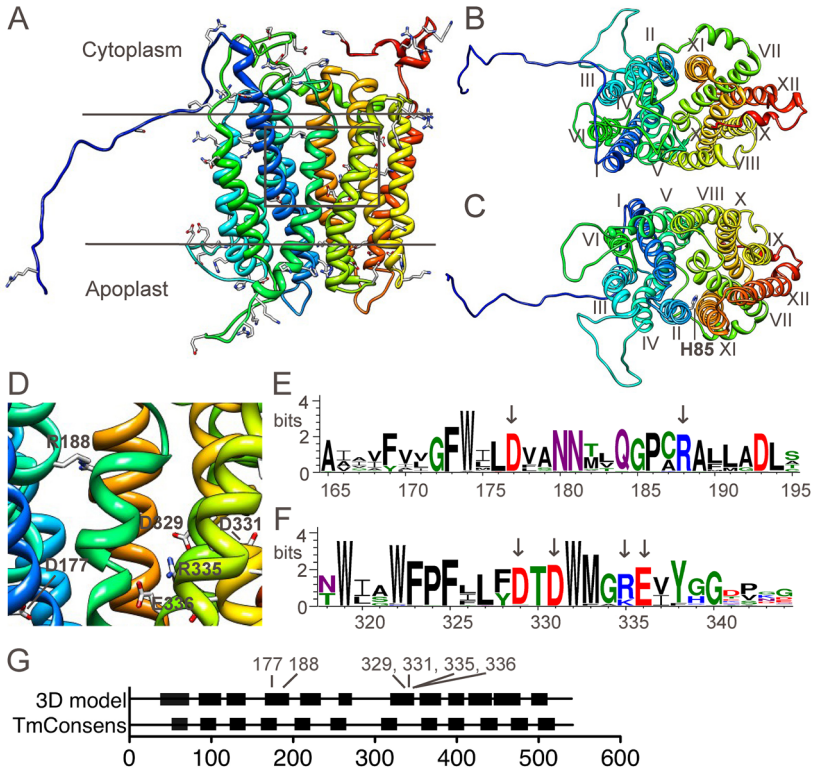

Figure 1. Predicted 3D model of OsSUT1. (A) Ribbon representation of the OsSUT1 model viewed parallel to the membrane. Twelve transmembrane helices were colored from the N-terminus (blue) to the C-terminus (red). Charged amino acids are highlighted by presentation of their side chains. (B) OsSUT1 model viewed from the cytoplasmic side. (C) OsSUT1 model viewed from the extracellular side. Residue His85, equivalent to His65 in AtSUC1,[18] is labeled at the extracellular end of helix II. (D) Close-up of charged amino acids in transmembrane helices. The six amino acids analyzed in this study are labeled. (E and F) Amino acid sequence conservation in predicted helices IV and VII, respectively. The six candidate amino acids are indicated by arrows. (G) Comparison of OsSUT1 transmembrane helices based on the 3D model and based on TmConsens, a consensus of 18 individual secondary structural predictions (http://aramemnon.botanik.uni-koeln.de). The numbers above the diagram refer to amino acid positions mutated in this study.

acids within membrane spans are important for transport activity.

EXPERIMENTAL PROCEDURES

3D Structure Modeling. A dendrogram of GlpT (PDB entry 1pw4), EmrD (PDB entry 2gfp), and LacY (PDB entry 1pv7) was calculated with MODELLER.[35] Then an iterative pairwise alignment of most closely related subalignments was generated on the basis of dynamic programming using the BLOSUM62 matrix. This alignment incorporated structural information about the templates by setting gap penalties that strongly discourage insertion of gaps in known secondary structures (e.g., helices). The query sequence (OsSUT1) was then mapped to existing structures of the templates to produce a sequence-to-structure alignment. In regions where no template was available, atoms were arranged to minimize the global energy and to satisfy stereochemical restraints.

Molecular Biology. Mutagenesis of OsSUT1 in pCR8/GW (Invitrogen) was performed using the QuikChange II site-directed mutagenesis kit (Stratagene) with 8% dimethyl sulfoxide (DMSO) in the polymerase chain reactions. For GFP fusions, eGFP was amplified and inserted into the ApaI site before the attRI site in the pOO2/GW vector to yield the pOO2GFP/GW vector. For expression in oocytes, OsSUT1 wild-type and its mutants in pCR8/GW were recombined with pOO2/GW and pOO2GFP/GW. cRNA was prepared using the SP6 mMessage mMachine kit (Ambion). For expression in yeast, OsSUT1 wild-type and its mutants in pCR8/GW were recombined with pDR196/GW.

Oocyte Electrophysiology. *Xenopus laevis* oocytes were prepared as previously described.[31,36] Modified Na-Ringer solution [115 mM NaCl, 2 mM KCl, 1.8 mM $CaCl_2$, 1 mM $MgCl_2$, and 5 mM MES-Tris (pH 5.6)] was used in all assays as the oocyte bath solution. Two-electrode voltage clamp recordings (TEVC) were made with a TEV 200A amplifier (Dagan). From a holding potential of −40 mV, voltage pulses from −157 to 58 mV were applied for 203 ms. Steady-state currents are presented as the mean current between 150 and 200 ms following the onset of voltage pulses. Sucrose-induced currents were obtained by subtracting an average of baseline currents before and after the application of substrate.

[^{14}C]Sucrose Uptake. *Saccharomyces cerevisiae* (baker's yeast) strain SEY6210 (Matα ura3-52 leu2-3, 112 his3-Δ200 trp1-Δ901 lys2-801 suc2-Δ9) was transformed with pDR196/GW containing wild-type OsSUT1, mutants, or the empty vector. Yeast cells were grown in SD-ura medium (1.7 g/L yeast nitrogen base, 5 g/L ammonium sulfate, 20 g/L glucose, and appropriate supplements) to an OD_{600} of 1.0, harvested by centrifugation, and resuspended in 25 mM NaH_2PO_4 (pH 4.0) to a final OD_{600} of 20. Glucose (final concentration of 10 mM) was added to 60 μL of yeast cells 2 min before the uptake experiments. The assays were initiated by the addition of sucrose at either 4.6 μM or 1 mM (final concentration) and at 0.3 μCi/72 μL reaction volume. After incubation at 30 °C for 5 min, 50 μL of yeast cells was collected by vacuum filtration on

dx.doi.org/10.1021/bi201934h | *Biochemistry* 2012, 51, 3284−3291

glass fiber filters (Pall Corp.) and washed three times with 10 mM ice-cold sucrose. Radioactivity retained on filters was counted using a liquid scintillation counter.

RESULTS

Prediction of an OsSUT1 Structural Model. The OsSUT1 protein sequence (Os03g07480) was used to query the Protein Homology/analogY Recognition Engine (PHYRE)[35] to search for structural prediction templates. The top three hits were MFS proteins GlpT (PDB entry 1pw4), EmrD (PDB entry 2gfp), and LacY (PDB entry 1pv7). The level of amino acid identity among LacY, GlpT, EmrD, and OsSUT1 is low (10−15%); however, 3D structures of the first three proteins have been determined to be very similar.[20−22,25] To test the ability of the 3D structure prediction software MODELLER[37] to predict MFS structures, we used LacY as the template to build a model of GlpT and superimposed it with the crystal structure of GlpT. The crystal structure and the predicted GlpT structure were very similar. The ability of MODELLER to predict the GlpT structure indicated that prediction of the OsSUT1 structure using MFS templates might be possible even though the level of sequence identity to proteins of known structure was low.

Amino acid sequences of LacY, GlpT, and EmrD were used to generate a multiple-template alignment for homologue modeling via MODELLER. The reliability of produced 3D models was validated by ProQ[38] and via evaluation of scores generated from MODELLER. The highest-scoring model [id B99990031 (Figure 1)] was selected to represent the general structure of OsSUT1. 3D models were built using LacY, GlpT, and EmrD as single templates, as well. The 3D model from the multiple-sequence alignment is presented here. It has been reported that multiple-sequence templates improve the quality of comparative structure models through better coverage when aligned to different domains of the target, and by providing choices of the best local template when aligned to the same target region.[39]

In agreement with previously envisioned SUT structures,[40−42] the 3D model of OsSUT1 is composed of two six-helix bundles surrounding a hydrophilic cavity. Both the N- and C-termini and a central loop are located in the cytoplasm (Figure 1A−C). Major differences exist between this model and previous topology models based on hydropathy analysis regarding the length of membrane-spanning domains; some helices in the 3D model are longer, with a corresponding decrease in the size of connecting loops (Figure 1G). This changes the position, relative to the membrane, of many amino acids.

In the predicted OsSUT1 model, the arrangement of transmembrane spans is similar to that of the template structures.[19−23] Helices I, II, IV, V, VII, VIII, X, and XI form the central cavity, the proposed translocation pathway for substrates. MFS signature motifs (RXXXR)[40,43] were assigned to the loop 2−3/helix III interface and loop 8−9 (residues K116−R120 and R382−R387, respectively). His85, equivalent to His65 in AtSUC1,[18] is located in extracellular loop 1−2 in the model (Figure 1C). When all charged amino acids are displayed (Figure 1A), it is clear that most of them are located outside of the membrane in extracellular or cytoplasmic loops. However, several charged amino acids are located within transmembrane helices, surrounding the central cavity (Figure 1A,D), indicating potentially important roles. Six of these charged amino acids are highly conserved within SUT proteins (Figure 1E,F). In an alignment of 43 plant SUT proteins, Asp177, Arg188, Asp331, and Glu336 are 100% conserved. Asp329 is conserved in all but two SUTs. Arg335 is present in 79% of SUT proteins, with lysine at the same position in the remaining 21% of the SUT proteins (Figure 1E,F).

Analysis of OsSUT1 Mutants. The six charged amino acids (Figure 1D−G) were mutated individually, and the activity of the mutated transporters was assayed. Asp177, Asp329, and Asp331 were changed to asparagine; Arg188 was changed to lysine, and Glu336 was changed to glutamine. Arg335 was replaced with histidine because lysine is present at this position in some homologues (Figure 1F). The electrophysiological assay[3,5,44] used in this study depends on the localization of the wild-type and mutant forms of OsSUT1 in the plasma membrane of *X. laevis* oocytes. To determine if protein localization was affected by mutagenesis, N-terminal GFP fusions were made for the wild type and six mutants. Transport activities of the GFP fusions were measured by TEVC, and cellular localization was analyzed by confocal laser scanning microscopy. Transport activities of wild-type OsSUT1 and its mutants without GFP fusion were also measured by expression in oocytes and yeast.

Uninjected oocytes had no detectable sucrose-induced currents (Figure 2A) as previously shown.[44] GFP-OsSUT1 was functional when expressed in oocytes. Application of 30 mM sucrose produced an inward-directed current (Figure 2B), consistent with the coupled transport of H^+.[31] No sucrose-induced currents were observed for either D177N or D331N

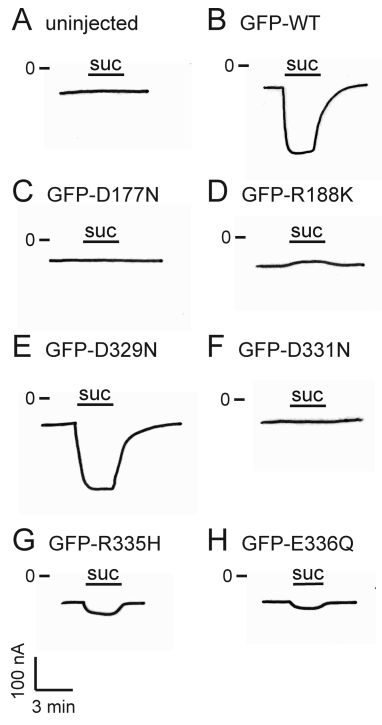

Figure 2. Two-electrode voltage clamp recordings of oocytes expressing wild-type GFP-OsSUT1 and its mutants. (A) Uninjected oocyte control. (B) Representative sucrose-induced current in an oocyte expressing wild-type GFP-OsSUT1. (C−H) Sucrose-induced currents in oocytes expressing GFP-OsSUT1 mutants. Following cRNA injection, oocytes were incubated for 4 days before data were recorded. Oocyte membrane potentials were clamped at −40 mV, and currents were recorded. Sucrose (30 mM) in Na-Ringer solution was applied where indicated.

(Figure 2C,F). Furthermore, oocytes expressing either GFP-D177N or GFP-D331N showed no sucrose-induced current at any membrane potential tested (from −157 to 58 mV). Other substrates of wild-type OsSUT1, including maltose, salicin, and α-phenyl glucoside,[31] also failed to induce detectable currents in GFP-D177N- or GFP-D331N-expressing oocytes.

Only background fluorescence was detected in uninjected oocytes (Figure 3A). Oocytes expressing GFP-OsSUT1 showed a plasma membrane localization of GFP fluorescence (Figure 3B). The GFP fluorescence intensity and localization in oocytes expressing GFP-D177N (Figure 3C) and GFP-D331N (Figure 3F) were indistinguishable from that in oocytes expressing GFP-OSUT1 (Figure 3B). This indicated that these single-amino acid substitutions did not affect membrane localization, and that the lack of measurable sucrose-induced current was due to changes in the function of the transporter. To exclude an effect of the GFP fusion on OsSUT1 function, additional transport experiments were conducted with OsSUT1 transporters lacking GFP fusions. When measured under the same conditions, oocytes expressing wild-type OsSUT1 exhibited large inward currents (Figure 4B), while uninjected oocytes or those expressing D177N or D331N showed no detectable current (Figure 4B).

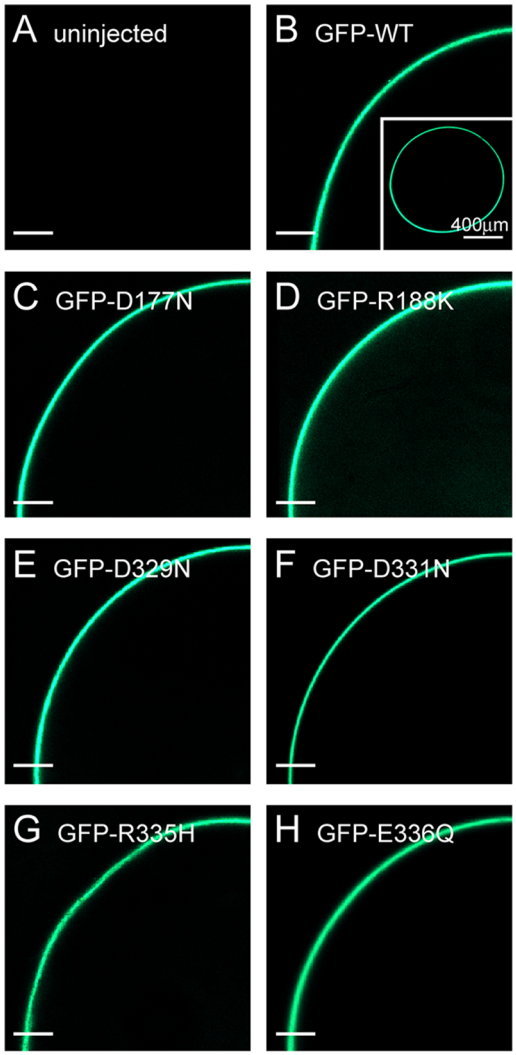

Figure 3. Confocal images of oocytes showing plasma membrane localization. (A) Uninjected oocyte. (B) Oocyte expressing wild-type GFP-OsSUT1. (C−H). Oocytes expressing GFP-OsSUT1 mutants. Images were captured using a Nikon Eclipse C1 confocal laser scanning microscope, with an excitation wavelength of 488 nm, displaying a quarter of an optical slice of a 4 day postinjection oocyte. The inset in panel B shows an entire oocyte at a lower magnification. Scale bars represent 100 μm except as noted in the inset in panel B.

In oocyte electrophysiological assays, the coupling ion (H^+) current was measured. To exclude the possibility that the OsSUT1 mutants transported sucrose but not H^+, [^{14}C]sucrose uptake was assessed in yeast (*Saccharomyces cerevisiae*) strain SEY6210 expressing wild-type OsSUT1 or its mutants. Yeast expressing D177N had no detectable [^{14}C]sucrose uptake when assays were performed at 1 mM sucrose (Figure 4A) or 4.6 μM sucrose (Figure 4D). Therefore, we conclude that the D177N mutant completely lacks sucrose transport activity. Yeast expressing D331N did not show [^{14}C]sucrose uptake that could be distinguished from the vector control at 1 mM sucrose. However, at a high specific activity (4.6 μM sucrose), D331N showed a measurably higher level (P value of 0.0022) of [^{14}C]sucrose uptake. This represents 2.3% of the wild-type activity at this sucrose concentration. It is likely that transport of sucrose by D331N was uncoupled from H^+ transport because no sucrose-induced H^+ current was measured for this mutant and 2.3% of the wild-type sucrose-induced current is much greater than the limit of detection.

The R335H and E336Q mutants retained partial transport activity. In electrophysiological experiments, oocytes expressing GFP-R335H or GFP-E336Q exhibited smaller currents than the wild type (Figure 2G,H). GFP fusions of R335H or E336Q, when expressed in oocytes, showed no detectable difference in localization or intensity from wild-type GFP-OsSUT1 (Figure 3G,H). Smaller sucrose-induced currents were also observed when R335H and E336Q were not fused with GFP (Figure 4B). Consistent with these results, yeast expressing either R335H or E336Q showed compromised sucrose transport in ^{14}C-labeled sucrose uptake assays (Figure 4A).

To explore the transport deficiencies of R335H and E336Q mutants, we measured their transport kinetics using electrophysiology. At a membrane potential of −118 mV and at pH 5.6, the $K_{0.5}$ of E336Q for sucrose was 10.42 mM, not significantly different from the wild-type value (P value of 0.075) (Table 1 and Figure 4C). The $K_{0.5}$ of R335H for sucrose was 15.46 mM, 2-fold higher than that of wild-type OsSUT1 (P value of <0.001) (Table 1 and Figure 4C). The V_{max} values for R335H and E336Q were −0.19 and −0.05 μA, respectively, significantly lower than that of the wild type (−0.46 μA) (Table 1 and Figure 4C).

The transport activity of the D329N mutant was similar to that of the wild type. Asp329 is highly conserved and close to Asp331 (Figure 1F), yet the replacement of Asp329 with asparagine did not affect sucrose transport. When expressed in oocytes, D329N fused with GFP (Figure 2E) or without GFP (Figure 4B) produced sucrose-induced inward currents similar to that of the wild type. The $K_{0.5}$ and V_{max} values of D329N were 6.47 mM and −0.60 μA, respectively (Figure 4C and Table 1), showing no significant difference from those of the wild type. When the D329N mutant was expressed in yeast, its [^{14}C]sucrose uptake rate [1.04 nmol (10^8 cells)$^{-1}$ (5 min)$^{-1}$] was not significantly different than that of the wild type [1.90 nmol (10^8 cells)$^{-1}$ (5 min)$^{-1}$; P value of 0.151] (Figure 4A). These results suggested that Asp329 of OsSUT1 was relatively less important for transport activity than Asp177 or Asp331.

dx.doi.org/10.1021/bi201934h | *Biochemistry* 2012, 51, 3284−3291

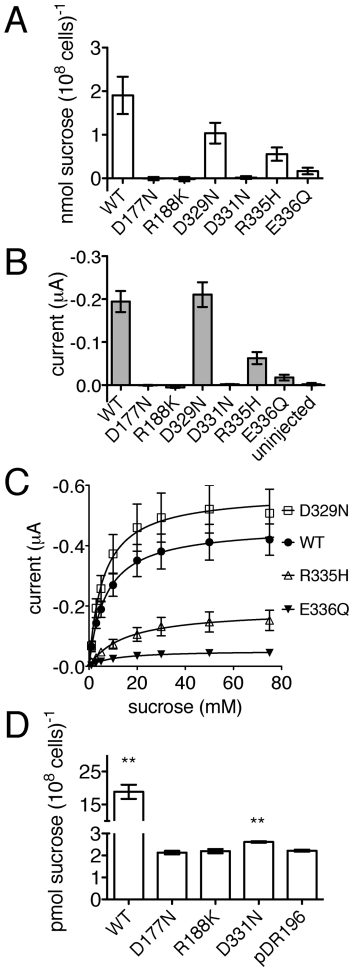

Figure 4. Transport of sucrose by wild-type OsSUT1 and its mutants. (A) Uptake of [^{14}C]sucrose by yeast SEY6210 expressing OsSUT1 constructs without GFP. Assays were performed at 30 °C with 1 mM sucrose in sodium phosphate buffer (pH 4.0) for 5 min. Background uptake [0.498 ± 0.072 nmol $(10^8$ cells$)^{-1}$ (5 min)$^{-1}$] by yeast transformed with the empty vector (pDR196) was subtracted from the uptake value of each construct. Each bar represents three replicates for each construct, using independent yeast transformants. Data are presented as means ± the standard error (SE) (n = 3). (B) Sucrose-induced currents in oocytes expressing OsSUT1 constructs without GFP. Oocytes were voltage clamped at −40 mV, and mean currents induced by 30 mM sucrose (background subtracted) are presented as means ± SE. At least three oocytes from different batches were tested for each construct. (C) Kinetics of transport of sucrose by oocytes expressing wild-type OsSUT1 and three mutants. Sucrose-induced currents were measured at −118 mV and plotted vs substrate concentration. Currents fit to the Michaelis−Menten equation are shown (curved lines). Values correspond to means ± SE (n = 4−6 oocytes). Error bars of D329N and the wild type partially overlap; some error bars (E336Q) are hidden by the symbols. (D) Uptake of [^{14}C]sucrose at high specific activities by yeast expressing OsSUT1 mutants. Conditions were the same as for panel A, except the final sucrose concentration was 4.6 μM and the background uptake by empty vector pDR196 was not subtracted. Data are presented as means ± SE (n = 3 independent transformants). Means were compared to the vector control using a two-sided Student's t test, and two asterisks indicate a P value of <0.01.

Arg188 is a positively charged residue located in the same helix as Asp177 (helix IV). Like in the case of D177N and D331N, when R188K was expressed in oocytes, sucrose-induced inward currents were not observed. However, the R188K mutant showed a unique response; when sucrose was applied, a decrease in inward current was observed (Figures 2D and 4B). On average, 30 mM sucrose triggered a 0.0058 μA (n = 6) decrease in inward currents in oocytes expressing R188K (Figure 4B). When expressed in yeast, R188K did not confer [^{14}C]sucrose uptake activity at either 1 mM sucrose (Figure 4A) or 4.6 μM sucrose (Figure 4D). This indicates that R188K retains the ability to bind sucrose but completely lacks sucrose transport activity. The decrease in inward current observed upon sucrose application is most likely due to the blockage of H^+ leakage current through the R188K mutant transporter.

Table 1. Sucrose Transport Kinetics of Wild-Type OsSUT1 and Three Mutants Measured by Two-Electrode Voltage Clamping[a]

	$K_{0.5}$ for sucrose (mM)		V_{max} (μA)		
construct	mean ± SE	P value	mean ± SE	P value	n
wild-type	7.08 ± 1.10		−0.46 ± 0.06		4
D329N	6.47 ± 0.59	0.648	−0.60 ± 0.10	0.290	5
R335H	15.46 ± 1.16	0.001	−0.19 ± 0.04	0.012	6
E336Q	10.42 ± 1.16	0.075	−0.05 ± 0.01	0.006	5

[a]Means for $K_{0.5}$ and V_{max} values are from experiments described in Figure 4C. Two-sided t tests were performed between the wild type and each mutant, with corresponding P values listed.

DISCUSSION

Features of the 3D Model. The presence of charged amino acids within transmembrane spans in MFS proteins is known to interfere with topology predictions using hydropathy analysis. Glu126 and Arg144 of LacY, initially placed at the membrane solution interface by hydropathy profiling,[45,46] are located within transmembrane spans.[20] Similarly, the membrane topology of OsSUT1 based on the 3D model is quite different from conventional transmembrane predictions (Figure 1G). Five of six charged amino acids located in transmembrane helices in the model (Figure 1A,D) were found to be important for OsSUT1 function (Figures 2 and 4). This is consistent with the presence of irreplaceable charged amino acid residues within transmembrane spans in LacY.

Transmembrane span lengths in the 3D structural prediction for OsSUT1 (mean of 27.5 amino acids) are longer than those generated by traditional transmembrane span prediction programs [mean of 21.0 amino acids (Figure 1G)]. The average number of amino acids in membrane spans of existing MFS crystal structures[20−23] is 26 (PDB entries 1pv7, 1pw4, 2gfp, and 307p). Moreover, all except one or two membrane spans from each of the MFS crystal structures are longer than 20 amino acids (PDB entries 1pv7, 1pw4, 2gfp, and 307p). Longer transmembrane spans are necessary to account for tilted helices and to allow helices the flexibility to bend in the membrane and to interact with one another during the substrate translocation process.[20]

Potential Roles of Key Amino Acids. During the LacY substrate binding process, the OH groups at positions 2−4 and 6 of the galactosyl ring of lactose are determinant.[47,48] It has been shown that for substrate recognition by SUTs, the glucosyl moiety is required[44] and the OH groups at positions 2−4 and 6 of the glucosyl ring of sucrose are essential.[49,50] Most amino acids critical for LacY substrate binding are in the N-terminal half, whereas residues responsible for H^+ translocation are in the C-terminal half.[20] Because of the structural similarity of lactose and sucrose, and the similarity of LacY and

dx.doi.org/10.1021/bi201934h | Biochemistry 2012, 51, 3284−3291

SUTs, it is reasonable to predict that basic similarities exist in their transport mechanisms. Accordingly, essential amino acids in the N-terminal half of SUTs might be responsible for sugar recognition, while key residues in the C-terminal half may be involved in H^+ transport.

The substrate binding of LacY largely relies on Arg144 in helix V, located close to the cytoplasmic side.[20,46] Even the most conservative substitution (R144K) abolished lactose transport activity.[27] The two guanidine NH_2 groups of Arg144 form a bifurcated hydrogen bond with C_3 and C_4 hydroxyl OH groups of the lactose galactosyl ring; one of the NH_2 groups also interacts with either Glu269 or Glu126.[20,26,47] In our 3D model, Arg188 of OsSUT1 corresponds to Arg144 of LacY in many respects. Arg188 from helix IV was located relatively close to the cytoplasmic half (Figure 1D), and the replacement of Arg188 with Lys caused a loss of transport activity similar to that experienced by LacY(R144K) (Figure 4A,B). The application of sucrose to oocytes expressing R188K resulted in a small decrease in inward current (Figure 2D). This indicated that OsSUT1(R188K) has a H^+ leak in the absence of substrate. This leak is larger than that observed in wild-type SUTs. For example, application of the competitive inhibitor sucralose to ShSUT1 (from sugar cane) does not result in an apparent decrease in inward current.[51] Therefore, in the OsSUT1(R188K) mutant, there is apparently a defect that increases H^+ translocation in the absence of substrate while preventing coupled H^+/sucrose transport even though the mutant binds sucrose. We suggest that Arg188 forms a hydrogen bond with one or more OH groups of sucrose. The R188K mutant can bind sucrose, but translocation is blocked. In addition, conformational differences in the R188K mutant result in the H^+ leak.

Glu126 of LacY, initially placed at the membrane−water interface of LacY by hydropathy profiling,[45,46] is located in helix IV of LacY.[20] The replacement of Glu126 with glutamine resulted in a strongly decreased rate of transport of lactose.[27] Further studies illustrate that this residue is directly involved in lactose binding and recognition.[46] In the crystal structure of LacY, Glu126 is near Arg144 and may interact with the substrate via water molecules.[20] In OsSUT1, Asp177 is located in the equivalent helix (IV) and has the same charge as Glu126 of LacY. We suggest that Asp177 may participate in substrate binding. The change of Asp177 to asparagine resulted in a complete loss of sucrose transport (Figure 2C and 4A,B,D).

Like Glu269, Arg302, His322, and Glu325 in the C-terminal half of LacY,[52−56] Asp331, Arg335, and Glu336 in the C-terminal half of OsSUT1 might be involved in H^+ transport. Mutation of Asp331 to Asn in OsSUT1 resulted in the complete loss of H^+ translocation, while only 2.3% of [^{14}C]sucrose uptake activity remained. This raises the possibility that Asp331 may function like Glu325 and Glu269, which are required for H^+ translocation relay in LacY.[52,53,56] Further experiments, such as measurement of counterflow in membrane vesicles, will be needed to test this hypothesis. Asp329 of OsSUT1 might not be as crucial, because the transport activity of D329N was not significantly different from that of the wild type (Figures 2E and 4). It is likely that additional amino acids not addressed in this study, for example, polar but uncharged and nonpolar amino acids in the transmembrane helices, also are involved in sucrose binding and H^+ translocation. On the basis of the results presented here, LacY and SUTs both contain important charged amino acids within transmembrane spans. Further work will be required to determine if there are additional similarities in the transport mechanism.

Previous site-directed mutagenesis analysis of SUTs was limited to the His65 studies.[18] Because the conservative H65R and H65K mutants of AtSUC1 are more active than the wild type,[18] His65 of AtSUC1 is not considered essential for activity. In this paper, we reported a 3D model for OsSUT1 generated using multiple structures of MFS proteins as templates. On the basis of the 3D model, six conserved charged amino acids within membrane spans were identified. Through mutagenesis studies, we showed that conservative mutation of five of those six amino acids strongly affected transport activity. Future investigations are needed to discover other key amino acids, to reveal the translocation mechanism, and to determine the protein structure of SUTs.

AUTHOR INFORMATION

Corresponding Author

*Address: 250 Biological Sciences, 1445 Gortner Ave., St. Paul, MN 55108. Telephone: (612) 625-4763. Fax: (612) 625-1738. E-mail: jward@umn.edu.

Funding

Supported by the Division of Chemical Sciences, Geosciences, and Biosciences, Office of Basic Energy Sciences, of the U.S. Department of Energy (Grant DE-FG02-10ER15886 to J.M.W.).

Notes

The authors declare no competing financial interest.

ACKNOWLEDGMENTS

We thank Christopher Kauffman (Computer Science/Engineering, University of Minnesota) for recommendations about structure prediction programs. We also thank Mark Sanders (Imaging Center, College of Biological Sciences, University of Minnesota) for instruction in confocal laser scanning microscopy.

ABBREVIATIONS

OsSUT1, rice sucrose transporter 1; AtSUC1, *Arabidopsis* sucrose transporter 1; MFS, major facilitator superfamily; SUT, sucrose transporter; 3D, three-dimensional; DEPC, diethyl pyrocarbonate; GFP, green fluorescence protein; OxlT, oxalate/formate antiporter; LacY, lactose permease; GlpT, glycerol-3-phosphate transporter; EmrD, multidrug transporter; FucP, fucose proton symporter; TEVC, two-electrode voltage clamp; PHYRE, Protein Homology/analogY Recognition Engine; PDB, Protein Data Bank.

REFERENCES

(1) Bush, D. R. (1990) Electrogenicity, pH-Dependence, and Stoichiometry of the Proton-Sucrose Symport. *Plant Physiol. 93*, 1590−1596.

(2) Carpaneto, A., Geiger, D., Bamberg, E., Sauer, N., Fromm, J., and Hedrich, R. (2005) Phloem-localized, proton-coupled sucrose carrier ZmSUT1 mediates sucrose efflux under the control of the sucrose gradient and the proton motive force. *J. Biol. Chem. 280*, 21437−21443.

(3) Boorer, K. J., Loo, D. D., Frommer, W. B., and Wright, E. M. (1996) Transport mechanism of the cloned potato H^+/sucrose cotransporter StSUT1. *J. Biol. Chem. 271*, 25139−25144.

(4) Slone, J. H., Buckhout, T. J., and Vanderwoude, W. J. (1991) Symport of proton and sucrose in plasma membrane vesicles isolated from spinach leaves. *Plant Physiol. 96*, 615−618.

(5) Zhou, J., Theodoulou, F., Sauer, N., Sanders, D., and Miller, A. J. (1997) A kinetic model with ordered cytoplasmic dissociation for SUC1, an *Arabidopsis* H^+/sucrose cotransporter expressed in *Xenopus* oocytes. *J. Membr. Biol. 159*, 113−125.
(6) Gottwald, J. R., Krysan, P. J., Young, J. C., Evert, R. F., and Sussman, M. R. (2000) Genetic evidence for the in planta role of phloem-specific plasma membrane sucrose transporters. *Proc. Natl. Acad. Sci. U.S.A. 97*, 13979−13984.
(7) Riesmeier, J. W., Willmitzer, L., and Frommer, W. B. (1994) Evidence for an essential role of the sucrose transporter in phloem loading and assimilate partitioning. *EMBO J. 13*, 1−7.
(8) Slewinski, T. L., Meeley, R., and Braun, D. M. (2009) Sucrose transporter 1 functions in phloem loading in maize leaves. *J. Exp. Bot. 60*, 881−892.
(9) Burkle, L., Hibberd, J. M., Quick, W. P., Kuhn, C., Hirner, B., and Frommer, W. B. (1998) The H^+-sucrose cotransporter NtSUT1 is essential for sugar export from tobacco leaves. *Plant Physiol. 118*, 59−68.
(10) Harada, M., Li, Y. F., El-Gamil, M., Rosenberg, S. A., and Robbins, P. F. (2001) Use of an in vitro immunoselected tumor line to identify shared melanoma antigens recognized by HLA-A*0201-restricted T cells. *Cancer Res. 61*, 1089−1094.
(11) Inagaki, K., Suzuki, T., Ito, S., Suzuki, N., Adachi, K., Okuyama, T., Nakata, Y., Shimizu, H., Matsuura, H., Oono, T., Iwamatsu, H., Kono, M., and Tomita, Y. (2006) Oculocutaneous albinism type 4: Six novel mutations in the membrane-associated transporter protein gene and their phenotypes. *Pigm. Cell Res. 19*, 451−453.
(12) Mariat, D., Taourit, S., and Guerin, G. (2003) A mutation in the MATP gene causes the cream coat colour in the horse. *Genet. Sel. Evol. 35*, 119−133.
(13) Newton, J. M., Cohen-Barak, O., Hagiwara, N., Gardner, J. M., Davisson, M. T., King, R. A., and Brilliant, M. H. (2001) Mutations in the human orthologue of the mouse underwhite gene (uw) underlie a new form of oculocutaneous albinism, OCA4. *Am. J. Hum. Genet. 69*, 981−988.
(14) Costin, G. E., Valencia, J. C., Vieira, W. D., Lamoreux, M. L., and Hearing, V. J. (2003) Tyrosinase processing and intracellular trafficking is disrupted in mouse primary melanocytes carrying the underwhite (uw) mutation. A model for oculocutaneous albinism (OCA) type 4. *J. Cell Sci. 116*, 3203−3212.
(15) Fukamachi, S., Shimada, A., and Shima, A. (2001) Mutations in the gene encoding B, a novel transporter protein, reduce melanin content in medaka. *Nat. Genet. 28*, 381−385.
(16) Meyer, H., Vitavska, O., and Wieczorek, H. (2011) Identification of an animal sucrose transporter. *J. Cell Sci. 124*, 1984−1991.
(17) Lemoine, R. (2000) Sucrose transporters in plants: Update on function and structure. *Biochim. Biophys. Acta 1465*, 246−262.
(18) Lu, J. M., and Bush, D. R. (1998) His-65 in the proton-sucrose symporter is an essential amino acid whose modification with site-directed mutagenesis increases transport activity. *Proc. Natl. Acad. Sci. U.S.A. 95*, 9025−9030.
(19) Hirai, T., Heymann, J. A., Shi, D., Sarker, R., Maloney, P. C., and Subramaniam, S. (2002) Three-dimensional structure of a bacterial oxalate transporter. *Nat. Struct. Biol. 9*, 597−600.
(20) Abramson, J., Smirnova, I., Kasho, V., Verner, G., Kaback, H. R., and Iwata, S. (2003) Structure and mechanism of the lactose permease of *Escherichia coli*. *Science 301*, 610−615.
(21) Huang, Y., Lemieux, M. J., Song, J., Auer, M., and Wang, D. N. (2003) Structure and mechanism of the glycerol-3-phosphate transporter from *Escherichia coli*. *Science 301*, 616−620.
(22) Yin, Y., He, X., Szewczyk, P., Nguyen, T., and Chang, G. (2006) Structure of the multidrug transporter EmrD from *Escherichia coli*. *Science 312*, 741−744.
(23) Dang, S., Sun, L., Huang, Y., Lu, F., Liu, Y., Gong, H., Wang, J., and Yan, N. (2010) Structure of a fucose transporter in an outward-open conformation. *Nature 467*, 734−738.
(24) Guan, L., and Kaback, H. R. (2006) Lessons from lactose permease. *Annu. Rev. Biophys. Biomol. Struct. 35*, 67−91.
(25) Abramson, J., Kaback, H. R., and Iwata, S. (2004) Structural comparison of lactose permease and the glycerol-3-phosphate antiporter: members of the major facilitator superfamily. *Curr. Opin. Struct. Biol. 14*, 413−419.
(26) Kaback, H. R., Sahin-Toth, M., and Weinglass, A. B. (2001) The kamikaze approach to membrane transport. *Nat. Rev. Mol. Cell Biol. 2*, 610−620.
(27) Frillingos, S., Gonzalez, A., and Kaback, H. R. (1997) Cysteine-scanning mutagenesis of helix IV and the adjoining loops in the lactose permease of *Escherichia coli*: Glu126 and Arg144 are essential. *Biochemistry 36*, 14284−14290.
(28) Law, C. J., Almqvist, J., Bernstein, A., Goetz, R. M., Huang, Y., Soudant, C., Laaksonen, A., Hovmoller, S., and Wang, D. N. (2008) Salt-bridge dynamics control substrate-induced conformational change in the membrane transporter GlpT. *J. Mol. Biol. 378*, 828−839.
(29) Yousef, M. S., and Guan, L. (2009) A 3D structure model of the melibiose permease of *Escherichia coli* represents a distinctive fold for Na^+ symporters. *Proc. Natl. Acad. Sci. U.S.A. 106*, 15291−15296.
(30) Hirose, T., Imaizumi, N., Scofield, G. N., Furbank, R. T., and Ohsugi, R. (1997) cDNA cloning and tissue specific expression of a gene for sucrose transporter from rice (*Oryza sativa* L.). *Plant Cell Physiol. 38*, 1389−1396.
(31) Sun, Y., Reinders, A., LaFleur, K. R., Mori, T., and Ward, J. M. (2010) Transport activity of rice sucrose transporters OsSUT1 and OsSUT5. *Plant Cell Physiol. 51*, 114−122.
(32) Ohsugi, R., and Furbank, R. T. (2002) Antisense suppression of the rice sucrose transporter gene, OsSUT1, leads to impaired grain filling and germination but does not affect photosynthesis. *Funct. Plant Biol. 29*, 815−826.
(33) Scofield, G. N., Aoki, N., Hirose, T., Takano, M., Jenkins, C. L., and Furbank, R. T. (2007) The role of the sucrose transporter, OsSUT1, in germination and early seedling growth and development of rice plants. *J. Exp. Bot. 58*, 483−495.
(34) Scofield, G. N., Hirose, T., Aoki, N., and Furbank, R. T. (2007) Involvement of the sucrose transporter, OsSUT1, in the long-distance pathway for assimilate transport in rice. *J. Exp. Bot. 58*, 3155−3169.
(35) Bennett-Lovsey, R. M., Herbert, A. D., Sternberg, M. J., and Kelley, L. A. (2008) Exploring the extremes of sequence/structure space with ensemble fold recognition in the program Phyre. *Proteins 70*, 611−625.
(36) Reinders, A., Sivitz, A. B., Starker, C. G., Gantt, J. S., and Ward, J. M. (2008) Functional analysis of LjSUT4, a vacuolar sucrose transporter from *Lotus japonicus*. *Plant Mol. Biol. 68*, 289−299.
(37) Marti-Renom, M. A., Stuart, A. C., Fiser, A., Sanchez, R., Melo, F., and Sali, A. (2000) Comparative protein structure modeling of genes and genomes. *Annu. Rev. Biophys. Biomol. Struct. 29*, 291−325.
(38) Wallner, B., and Elofsson, A. (2003) Can correct protein models be identified? *Protein Sci. 12*, 1073−1086.
(39) Fernandez-Fuentes, N., Rai, B. K., Madrid-Aliste, C. J., Fajardo, J. E., and Fiser, A. (2007) Comparative protein structure modeling by combining multiple templates and optimizing sequence-to-structure alignments. *Bioinformatics 23*, 2558−2565.
(40) Ward, J. M., Kuhn, C., Tegeder, M., and Frommer, W. B. (1998) Sucrose transport in higher plants. *Int. Rev. Cytol. 178*, 41−71.
(41) Reinders, A., and Ward, J. M. (2001) Functional characterization of the α-glucoside transporter Sut1p from *Schizosaccharomyces pombe*, the first fungal homologue of plant sucrose transporters. *Mol. Microbiol. 39*, 445−454.
(42) Reinders, A., Schulze, W., Thaminy, S., Stagljar, I., Frommer, W. B., and Ward, J. M. (2002) Intra- and intermolecular interactions in sucrose transporters at the plasma membrane detected by the split-ubiquitin system and functional assays. *Structure 10*, 763−772.
(43) Pao, S. S., Paulsen, I. T., and Saier, M. H., Jr. (1998) Major facilitator superfamily. *Microbiol. Mol. Biol. Rev. 62*, 1−34.
(44) Chandran, D., Reinders, A., and Ward, J. M. (2003) Substrate specificity of the *Arabidopsis thaliana* sucrose transporter AtSUC2. *J. Biol. Chem. 278*, 44320−44325.
(45) Foster, D. L., Boublik, M., and Kaback, H. R. (1983) Structure of the lac carrier protein of *Escherichia coli*. *J. Biol. Chem. 258*, 31−34.

(46) Venkatesan, P., and Kaback, H. R. (1998) The substrate-binding site in the lactose permease of *Escherichia coli*. *Proc. Natl. Acad. Sci. U.S.A. 95*, 9802−9807.
(47) Sahin-Toth, M., Akhoon, K. M., Runner, J., and Kaback, H. R. (2000) Ligand recognition by the lactose permease of *Escherichia coli*: Specificity and affinity are defined by distinct structural elements of galactopyranosides. *Biochemistry 39*, 5097−5103.
(48) Sahin-Toth, M., Lawrence, M. C., Nishio, T., and Kaback, H. R. (2001) The C-4 hydroxyl group of galactopyranosides is the major determinant for ligand recognition by the lactose permease of *Escherichia coli*. *Biochemistry 40*, 13015−13019.
(49) Hitz, W. D., Card, P. J., and Ripp, K. G. (1986) Substrate recognition by a sucrose transporting protein. *J. Biol. Chem. 261*, 11986−11991.
(50) Griffin, S. D., Buxton, K. D., and Donaldson, I. A. (1993) The α-D-glucosyl C-2 hydroxyl is required for binding to the H^+-sucrose transporter in phloem. *Biochim. Biophys. Acta 1152*, 61−68.
(51) Reinders, A., Sivitz, A. B., Hsi, A., Grof, C. P., Perroux, J. M., and Ward, J. M. (2006) Sugarcane ShSUT1: Analysis of sucrose transport activity and inhibition by sucralose. *Plant, Cell Environ. 29*, 1871−1880.
(52) Ujwal, M. L., Sahin-Toth, M., Persson, B., and Kaback, H. R. (1994) Role of glutamate-269 in the lactose permease of *Escherichia coli*. *Mol. Membr. Biol. 11*, 9−16.
(53) Carrasco, N., Antes, L. M., Poonian, M. S., and Kaback, H. R. (1986) lac permease of *Escherichia coli*: Histidine-322 and glutamic acid-325 may be components of a charge-relay system. *Biochemistry 25*, 4486−4488.
(54) Puttner, I. B., Sarkar, H. K., Poonian, M. S., and Kaback, H. R. (1986) lac permease of *Escherichia coli*: Histidine-205 and histidine-322 play different roles in lactose/H^+ symport. *Biochemistry 25*, 4483−4485.
(55) Sahin-Toth, M., and Kaback, H. R. (2001) Arg-302 facilitates deprotonation of Glu-325 in the transport mechanism of the lactose permease from *Escherichia coli*. *Proc. Natl. Acad. Sci. U.S.A. 98*, 6068−6073.
(56) Franco, P. J., and Brooker, R. J. (1994) Functional roles of Glu-269 and Glu-325 within the lactose permease of *Escherichia coli*. *J. Biol. Chem. 269*, 7379−7386.